Myelin Basic Protein Interaction Landscape

Subjects: Biochemistry & Molecular Biology | Cell Biology
Contributor: Alexey Beogurov

Intrinsically disordered myelin basic protein (MBP) is one of the key autoantigens in autoimmune neurodegeneration and multiple sclerosis particularly. MBP is highly positively charged and lacks a distinct structure in solution, and therefore its intracellular partners are still mostly enigmatic. Here authors used combination of formaldehyde-induced cross-linking followed by immunoprecipitation and liquid chromatography-tandem mass spectrometry (LC-MS/MS) to elucidate the interaction network of MBP in mammalian cells and provide the list of potential MBP interacting proteins.

Keywords: myelin basic protein ; MBP ; interactome ; multiple sclerosis

1. Introduction

Myelinization of the axons is critical for the rapid conduction of the nerve impulses. Myelin is maintained as a tightly packed, lipid-rich multilayer membrane envelope to function as an electrical insulator. The importance of the myelin membrane is evident in terms of demyelinating diseases such as multiple sclerosis, which lead to severe neurological disability. Myelin is produced by specialized glial cells in both, central and peripheral nervous systems (CNS and PNS, respectively). Genetic abnormalities in myelin genes or an autoimmune destruction of myelin lead to severe neurological damage. Plenty of the lesions developed during dys- or demyelination processes can be associated with the partial violation of the tight interactions of myelin proteins with lipid bilayer. Myelin basic protein (MBP) is one of the most abundant among myelin proteins. It presents in high amount in CNS and PNS in oligodendrocytes and Schwann cells, respectively [1][2]. MBP is a peripheral membrane-associated semisubmersible protein with highly disordered structure in an aqueous solution [3][4][5]. However, number of data indicate that the interaction of MBP with ligands triggers the formation of secondary structures and some degree of MBP folding into a more compacted scaffold [6]. Aggarwal et al. showed that MBP controls biogenesis of myelin by weak forces emerging from MBP's inherent phase separation ability [7]. The interaction of MBP with the inner part of the membrane bilayer leads to charge neutralization and triggers its self-association into larger polymers and a phase transition to a dense protein network. The MBP interaction network has common features with the formation of amyloid fibrils [7]. This process occurs through phenylalanine-mediated hydrophobic and amyloid-like interactions, which provide the molecular basis for protein extrusion and "fastening" of myelin membranes. Data from Aggarwal et al. reveal the physico-chemical mechanism of how the cytosolic protein controls the morphology of complex membrane architecture [7]. Their results provide an explanation for the key mechanism of myelin membrane biogenesis with the possibility of using these data to suppress demyelinating diseases of the central nervous system.

MBP has many isoforms resulting from both alternative splicing and miscellaneous post-translational modifications [8]. It is present in the nervous system as isomers with different charge, and it is evident that charge-mediated effects modulate its function and interactions with ligands such as membrane surfaces [9][10][11][12]. Recently it was shown that MBP may be hydrolyzed by proteasome without ubiquitination [13] through novel class of Basic Elementary Autonomous Degrons (BEADs) interacting with PA28-capped proteasomes [14]. MBP is one of the major myelin sheath autoantigens in multiple sclerosis (MS) and animal models of autoimmune neurological disorders [15][16]. It is recognized [17] and cleaved [18][19] by autoantibodies and is efficient substrate for the immunoproteasome [20]. Post-translational modifications of MBP may play an important role in the pathogenesis of MS [21][22]. Removal of arginine occurs at several sites and has been increased in multiple sclerosis [21], and the degree of removal (or citrullination) of MBP correlates with the severity of multiple sclerosis [23]. In the study by Wang et al., recombinant murine analogs of two isoforms of the classic 18.5 kDa MBP, natural C1 and C8 charge isoforms (rmC1 and rmC2, respectively), were used as model proteins to elucidate the structure and function of charge isomers [24]. A number of biochemical and biophysical methods have been used to study the differences between the two isoforms in terms of structure and interaction with ligands, including calmodulin (CaM), various detergents, nucleotide analogs and lipids. In general, the results indicate that rmC8 in comparison with rmC1 is insufficient both in its structure and especially in function. Although the binding properties of CaM are very similar between the two forms, their interactions with membrane mimics were different. In addition, using fluorescently labeled nucleotides, MBP was observed

to bind to ATP and GTP, but not AMP; and this binding of nucleoside triphosphates was inhibited in the presence of CaM [24]. Recently it was shown that CaM may protect MBP from ubiquitin-independent proteasomal hydrolysis [25], which contributes to the development of autoimmune neurodegeneration [26].

2. Potential Binding Partners of MBP

To elucidate potential binding partners of MBP, we performed formaldehyde crosslinking, immunoprecipitation and mass spectrometry analysis of cell lysates of HEK293T cells overexpressing Flag-tagged human MBP (**Figure 1**). There are several reasons why we used HEK293T cells overexpressing Flag-tagged MBP: (i) There are only a few immortalized cell lines mimicking oligodendrocytes. Despite expression of surface markers similar to those of oligodendrocytes, they still do not fully represent native cells. (ii) Usage of primary oligodendroglial cultures is not obvious due to the heterogenicity and troubles with either transfection or transduction procedures. Finally, amount of endogenous MBP in native oligodendrocytes is dramatically high therefore it may effectively compete with recombinant tagged MBP, displacing it from protein complexes. (iii) Commercially available antibodies partially cross-react with eukaryotic proteome thus generating false-positive results. Additionally, usage of such low-affinity antibodies requires mild washing conditions in contrast to highly specific and affine anti-FLAG antibodies.

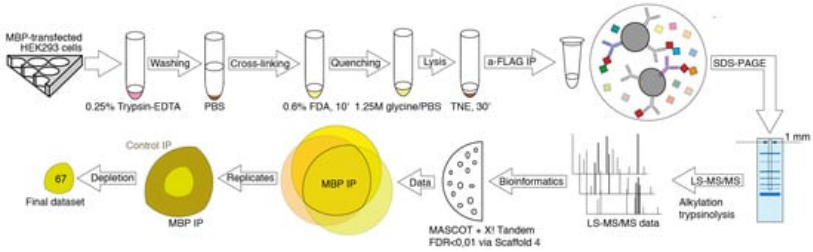

Figure 1. Experiment pipeline. HEK293T cells overexpressing Flag-tagged human MBP were detached, washed, and exposed to formaldehyde. The formaldehyde treated cells were washed and lysed in the mild conditions on ice. Protein complexes containing MBP were immunoprecipitated from the lysates using anti-Flag-agarose. The immunoprecipitated material was resolved by gradient SDS-PAGE. The cross-linked immunoprecipitated complexes were detected by Coomassie Blue staining. The 1 mm wide strips from the middle of each lane were cut and subjected to the in-gel-trypsinolysis procedure and mass spectrometry-based proteomics analysis. A total of three experiments were carried out with triplicate repeats in each.

MBP is characterized by multiple low-affinity semi-specific interactions and therefore combination of fixation of MBP-containing complexes by cross-linking and subsequent highly sensitive LC-MS/MS seems to be the most beneficial methodology. Despite the broad usage of formaldehyde as a crosslinking agent, studying of each particular protein requires optimization of experimental protocol due to the different protein environment, for example in case of cytosolic and membrane proteins [27]. In order to find the optimal conditions of the complex formation and low false-positive rate upon the use of formaldehyde as cross-linking reagent, we varied 2 out of 3 major parameters playing key role in formaldehyde cross-linking: the incubation time and the formaldehyde concentration. We excluded the temperature dependency from the analysis since the minimal effect of room temperature on the crosslinking efficiency was previously shown [28], and the use of other temperature ranges would introduce additional variability due to the difficulty of accurately following the crosslinking protocol. We analyzed the cross-linking efficiency in the range of formaldehyde concentrations from 0.4 to 1% and incubation time from 2 to 10 min and found that the optimal combination of parameters was 0.6% formaldehyde and 10 min of incubation time (data not shown). Upon these parameters, the size of the pool of formed complexes was in the range approximately from 50 to beyond 116 kDa (**Figure 2**A). It should be noted that under our conditions, the different incubation time in the range of 4–10 min did not result in significant changes in cross-linking. Thus, we chose the interval of 10 min, since it allowed us to minimize timing errors.

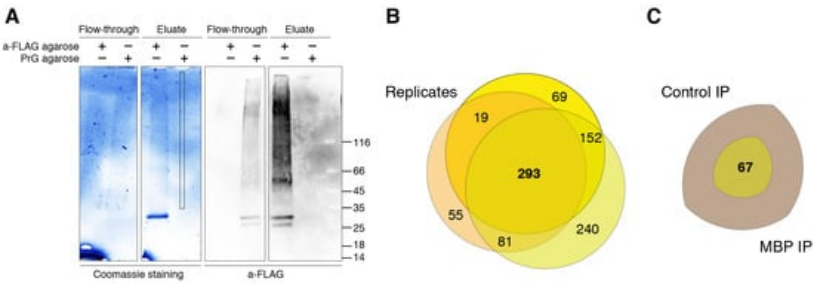

Figure 2. MBP immunoprecipitation and LS-MS/MS data. (**A**) Crosslinked MBP immunocomplexes resolved in gradient TGX Stain-Free Precast Gel (left) and immunostained with anti-Flag Ab (right). Analyzed zone is marked. (**B**) Venn diagram representing proteins identified in three experiments (with triplicate repeats in each) of immunoprecipitation against Flag-tagged human MBP. (**C**) Venn diagram representing unique and reproducible proteins identified in immunoprecipitation against Flag-tagged human MBP compared to negative control.

A total of three separate cross-linking-IP experiments were carried out with triplicate repeats in each to identify a pull of potential MBP interactors. As a negative control for the IP we used the same lysates and IP procedures, except protein A/G agarose beads (Thermo Fisher Scientific, Waltham, MA, USA) in the control IPs instead of anti-Flag agarose used in the MBP IPs. Final protocol used in the present study reads as follows. HEK293T cells overexpressing Flag-tagged human MBP were exposed to 0.6% formaldehyde for 10 min at room temperature (approximate 23 °C). The formaldehyde-treated cells were washed and lysed in the mild conditions on ice. To remove the lipids and DNA from obtained complexes the lysates were subjected to ultrasound and DNAse treatment. Protein complexes containing MBP were immunoprecipitated from the lysates and the immunoprecipitated complexes was resolved by gradient SDS-PAGE. The protein bands were stained by Coomassie Blue. The gel strips were exized and subjected to mass spectrometry-based proteomics analysis. Cross-linked complexes in a gradient gel gave an about even coloration in the 50-beyond 116 kDa range with several predominant bands (**Figure 2**A). Therefore, for MS analysis we excised a strip 1 mm wide from the middle of each lane starting from about 30 kDa and up to the top end of the separating gel. The strips were cut in 1 × 1 mm pieces and subjected to the in-gel-trypsinolysis procedure and subsequent MS analysis. Venn diagram in **Figure 2**B represents the distribution of the detected proteins between different experiments. The proteins, which were observed in at least two from three MBP IP experiments, and which were either not detected in three control experiments or whose Peptide-Spectrum Matches in MBP experiments were 3.5 or more times over those in control experiments, were considered as possible components of MBP-interacting network.

The detected MBP interactome included 67 different proteins that were identified by Mascot and/or X! Tandem with false discovery rate (FDR) for peptide-spectrum matches less than 0.01 determined by searching a reverse database (**Figure 2**C).

The analysis of identified proteins using String database showed that MBP interacts with eight major proteomic groups presented in **Table 1** and **Figure 3**.

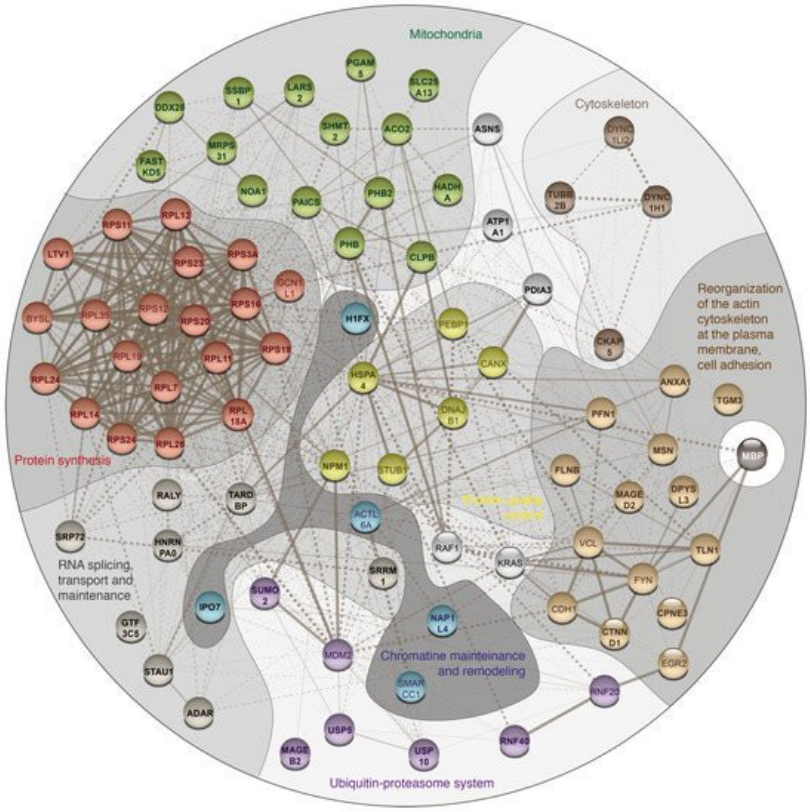

Figure 3. Atlas of the MBP intracellular partners visualized using String database [29][30]. Proteins identified in the current study are shown in bold.

Table 1. List of potential MBP interacting proteins. PSMs—Peptide-Spectrum Matches.

Protein Name	Gene Name	PSMs for MBP Experiment			PSMs for Control Experiment		
Protein synthesis							
40S ribosomal protein S16	RPS16	0	1	2	0	0	0
40S ribosomal protein S19	RPS19	0	1	1	0	0	0
40S ribosomal protein S20	RPS20	0	2	4	0	0	0
40S ribosomal protein S23	RPS23	3	0	4	0	0	0
60S ribosomal protein L11	RPL11	0	1	3	0	0	0
60S ribosomal protein L12	RPL12	0	1	1	0	0	0
60S ribosomal protein L18a	RPL18A	0	3	8	0	0	0
Protein LTV1 homolog	LTV1	0	2	1	0	0	0
Ribosomal protein L7, isoform CRA_a	RPL7	0	1	4	0	0	0
40S ribosomal protein S24	RPS24	0	2	3	0	0	1
40S ribosomal protein S11	RPS11	0	1	8	0	0	2
60S ribosomal protein L26	RPL26	0	3	6	0	0	2
40S ribosomal protein S3a	RPS3A	3	2	12	0	0	4
60S ribosomal protein L24	RPL24	0	2	2	0	0	1
60S ribosomal protein L14	RPL14	0	2	5	0	0	2
Mitochondria							
28S ribosomal protein S31, mitochondrial	MRPS31	0	2	2	0	0	0
Aconitate hydratase, mitochondrial	ACO2	1	0	2	0	0	0
cDNA FLJ46863 fis, clone UTERU3011558	NOA1	1	0	2	0	0	0
FAST kinase domain-containing protein 5, mitochondrial	FASTKD5	0	2	1	0	0	0
Isoform 2 of Caseinolytic peptidase B protein homolog	CLPB	0	2	8	0	0	0
Prohibitin (Fragment)	PHB1	2	2	3	0	0	0
Prohibitin-2	PHB2	5	2	6	0	0	0
Single-stranded DNA-binding protein, mitochondrial (Fragment)	SSBP1	1	0	2	0	0	0
Solute carrier family 25, member 13 (Citrin) variant (Fragment)	SLC25A13	0	1	3	0	0	0
Probable ATP-dependent RNA helicase DDX28	DDX28	0	2	6	0	0	1
Enoyl-CoA hydratase	HADHA	3	1	7	0	0	2
Probable leucine--tRNA ligase, mitochondrial	LARS2	0	2	3	0	0	1
AIR carboxylase (Fragment)	PAICS	2	0	6	0	0	2
Serine hydroxymethyltransferase	SHMT2	5	3	17	0	0	7
Serine/threonine-protein phosphatase PGAM5, mitochondrial	PGAM5	1	0	6	0	0	2
mRNA splicing, transport and maintenance							
cDNA FLJ77421, highly similar to Homo sapiens autoantigen p542 mRNA	RALY	2	1	0	0	0	0
Isoform 2 of General transcription factor 3C polypeptide 5	GTF3C5	0	2	1	0	0	0
Serine/arginine repetitive matrix 1 isoform 2 (Fragment)	SRRM1	0	4	1	0	0	0
Heterogeneous nuclear ribonucleoprotein A0	HNRNPA0	2	2	1	0	0	1

Protein Name	Gene Name	PSMs for MBP Experiment			PSMs for Control Experiment		
Signal recognition particle subunit SRP72	SRP72	1	0	4	0	0	1
cDNA FLJ75871, highly similar to Homo sapiens staufen, RNA binding protein (STAU), transcript variant T3, mRNA	STAU1	0	5	8	0	0	3
RNA-specific adenosine deaminase	ADAR	3	3	1	0	2	0
TAR DNA-binding protein 43	TARDBP	4	1	2	0	0	2
Reorganization of the cytoskeleton and intercellular adhesion							
Annexin A1	ANXA1	4	3	2	0	0	0
Catenin delta-1	CTNND1	0	1	5	0	0	0
Copine III, isoform CRA_a	CPNE3	0	2	2	0	0	0
Filamin B, beta (Actin binding protein 278), isoform CRA_a	FLNB	2	1	4	0	0	0
Moesin	MSN	2	0	8	0	1	1
cDNA FLJ56823, highly similar to Protein-glutamine gamma-glutamyltransferase E	TGM3	1	1	2	0	1	0
Profilin-1	PFN1	2	1	1	0	0	1
Talin-1	TLN1	3	4	16	0	1	5
Testicular secretory protein Li 7	DPYSL3	0	2	5	0	1	1
Cytoskeleton and intracellular traffic							
Cytoskeleton-associated protein 5	CKAP5	1	0	8	0	0	1
Cytoplasmic dynein 1 heavy chain 1	DYNC1H1	3	0	1	0	0	1
Tubulin beta chain	TUBB2B	0	2	5	0	0	2
Ubiquitin-proteasome system related							
cDNA, FLJ93871, highly similar to Homo sapiens melanoma antigen, family B, 2 (MAGEB2), mRNA	MAGEB2	0	1	3	0	0	0
E3 ubiquitin protein ligase	RNF40	0	2	1	0	0	0
Small ubiquitin-related modifier	SUMO2	0	2	2	0	0	0
Ubiquitin carboxyl-terminal hydrolase	USP10	0	2	1	0	0	0
Melanoma antigen family D, 2, isoform CRA_a	MAGED2	0	2	11	0	0	1
Ubiquitin carboxyl-terminal hydrolase	USP5	1	1	5	0	0	1
Quality control proteins							
Heat shock 70 kDa protein 4	HSPA4	2	0	1	0	0	0
Nucleophosmin (Fragment)	NPM1	11	3	6	0	0	3
Chromatin mainteinance and remodeling							
Nucleosome assembly protein 1-like 4, isoform CRA_b	NAP1L4	1	0	3	0	0	0
Histone H1.10	H1-10	2	1	0	0	0	0
Importin-7	IPO7	0	2	7	0	0	1
Unassigned to the specific group proteins							
Asparagine synthetase [glutamine-hydrolyzing]	ASNS	0	3	5	0	0	1
Protein disulfide-isomerase A3 (Fragment)	PDIA3	4	0	1	0	0	1
Sodium/potassium-transporting ATPase subunit alpha (Fragment)	ATP1A1	0	1	3	0	0	1

Protein Name	Gene Name	PSMs for MBP Experiment			PSMs for Control Experiment		
BAF53A protein	**BAF53A**	**2**	**0**	**1**	**0**	**0**	**0**
Peroxisome proliferator activated receptor interacting complex protein	**PRIC295**	**1**	**0**	**9**	**0**	**0**	**1**

Summarizing, elucidation of the mechanisms that guide myelin membrane biogenesis may result not only in deeper understanding of the pathogenesis of the autoimmune neurodegeneration, but also in the novel therapeutic approaches. Here using a combination of formaldehyde-induced cross-linking followed by immunoprecipitation and liquid chromatography-tandem mass spectrometry (LC-MS/MS) we showed that MBP interacts with eight major proteomic groups related to: (i) protein synthesis machinery; (ii) mitochondrial proteins, (iii) mRNA splicing, transport and maintenance, (iv) reorganization of the actin cytoskeleton at the plasma membrane and cell adhesion, (v) cytoskeleton and intracellular traffic, (vi) ubiquitin-proteasome system, (vii) protein quality control, and (viii) chromatin remodeling.

Elucidation of the mechanisms that guide myelin membrane biogenesis may result not only in deeper understanding of the pathogenesis of the autoimmune neurodegeneration, but also in novel therapeutic approaches. Here authors showed that MBP interacts not only with structural membrane-associated and cytoskeletal proteins, but also with proteins related to protein expression starting from transcription-translation machinery and continuing with mitochondrial proteins, transport and protein folding systems. Concluding, their data suggest that MBP may have not only a structural but also regulatory role in the myelinization process, which is significantly more proactive than was believed previously.

References

1. Benjamins, J.A.; Morell, P. Proteins of Myelin and Their Metabolism. Neurochem. Res. 1978, 3, 137–174.
2. Garbay, B.; Fournier, M.; Sallafranque, M.L.; Muller, S.; Boiron, F.; Heape, A.; Cassagne, C.; Bonnet, J. Po, MBP, Histone, and DNA Levels in Sciatic Nerve. Neurochem. Pathol. 1988, 8, 91–107.
3. Krigbaum, W.R.; Hsu, T.S. Molecular Conformation of Bovine A1 Basic Protein, a Coiling Macromolecule in Aqueous Solution. Biochemistry 1975, 14, 2542–2546.
4. Polverini, E.; Fasano, A.; Zito, F.; Riccio, P.; Cavatorta, P. Conformation of Bovine Myelin Basic Protein Purified with Bound Lipids. Eur. Biophys. J. EBJ 1999, 28, 351–355.
5. Harauz, G.; Ishiyama, N.; Hill, C.M.D.; Bates, I.R.; Libich, D.S.; Farès, C. Myelin Basic Protein-Diverse Conformational States of an Intrinsically Unstructured Protein and Its Roles in Myelin Assembly and Multiple Sclerosis. Micron 2004, 35, 503–542.
6. Harauz, G.; Libich, D. The Classic Basic Protein of Myelin—Conserved Structural Motifs and the Dynamic Molecular Barcode Involved in Membrane Adhesion and Protein-Protein Interactions. Curr. Protein Pept. Sci. 2009, 10, 196–215.
7. Aggarwal, S.; Snaidero, N.; Pähler, G.; Frey, S.; Sánchez, P.; Zweckstetter, M.; Janshoff, A.; Schneider, A.; Weil, M.-T.; Schaap, I.A.T.; et al. Myelin Membrane Assembly Is Driven by a Phase Transition of Myelin Basic Proteins Into a Cohesive Protein Meshwork. PLoS Biol. 2013, 11, e1001577.
8. Boggs, J.M. Myelin Basic Protein: A Multifunctional Protein. Cell. Mol. Life Sci. CMLS 2006, 63, 1945–1961.
9. Boggs, J.M.; Yip, P.M.; Rangaraj, G.; Jo, E. Effect of Posttranslational Modifications to Myelin Basic Protein on Its Ability to Aggregate Acidic Lipid Vesicles. Biochemistry 1997, 36, 5065–5071.
10. Bates, I.R.; Boggs, J.M.; Feix, J.B.; Harauz, G. Membrane-Anchoring and Charge Effects in the Interaction of Myelin Basic Protein with Lipid Bilayers Studied by Site-Directed Spin Labeling. J. Biol. Chem. 2003, 278, 29041–29047.
11. Hill, C.M.D.; Harauz, G. Charge Effects Modulate Actin Assembly by Classic Myelin Basic Protein Isoforms. Biochem. Biophys. Res. Commun. 2005, 329, 362–369.
12. Homchaudhuri, L.; Polverini, E.; Gao, W.; Harauz, G.; Boggs, J.M. Influence of Membrane Surface Charge and Post-Translational Modifications to Myelin Basic Protein on Its Ability to Tether the Fyn-SH3 Domain to a Membrane in Vitro. Biochemistry 2009, 48, 2385–2393.
13. Belogurov, A.; Kudriaeva, A.; Kuzina, E.; Smirnov, I.; Bobik, T.; Ponomarenko, N.; Kravtsova-Ivantsiv, Y.; Ciechanover, A.; Gabibov, A. Multiple Sclerosis Autoantigen Myelin Basic Protein Escapes Control by Ubiquitination during Proteasomal Degradation. J. Biol. Chem. 2014, 289, 17758–17766.

14. Kudriaeva, A.; Kuzina, E.S.; Zubenko, O.; Smirnov, I.V.; Belogurov, A. Charge-Mediated Proteasome Targeting. FASEB J. 2019, 33, 6852–6866.
15. Lutton, J.D.; Winston, R.; Rodman, T.C. Multiple Sclerosis: Etiological Mechanisms and Future Directions. Exp. Biol. Med. 2004, 229, 12–20.
16. Sospedra, M.; Martin, R. Immunology of Multiple Sclerosis. Annu. Rev. Immunol. 2005, 23, 683–747.
17. Belogurov, A.A.; Kurkova, I.N.; Friboulet, A.; Thomas, D.; Misikov, V.K.; Zakharova, M.Y.; Suchkov, S.V.; Kotov, S.V.; Alehin, A.I.; Avalle, B.; et al. Recognition and Degradation of Myelin Basic Protein Peptides by Serum Autoantibodies: Novel Biomarker for Multiple Sclerosis. J. Immunol. 1950 2008, 180, 1258–1267.
18. Ponomarenko, N.A.; Durova, O.M.; Vorobiev, I.I.; Belogurov, A.A.; Kurkova, I.N.; Petrenko, A.G.; Telegin, G.B.; Suchkov, S.V.; Kiselev, S.L.; Lagarkova, M.A.; et al. Autoantibodies to Myelin Basic Protein Catalyze Site-Specific Degradation of Their Antigen. Proc. Natl. Acad. Sci. USA 2006, 103, 281–286.
19. Ponomarenko, N.A.; Durova, O.M.; Vorobiev, I.I.; Belogurov, A.A.; Telegin, G.B.; Suchkov, S.V.; Misikov, V.K.; Morse, H.C.; Gabibov, A.G. Catalytic Activity of Autoantibodies toward Myelin Basic Protein Correlates with the Scores on the Multiple Sclerosis Expanded Disability Status Scale. Immunol. Lett. 2006, 103, 45–50.
20. Kuzina, E.S.; Chernolovskaya, E.L.; Kudriaeva, A.A.; Zenkova, M.A.; Knorre, V.D.; Surina, E.A.; Ponomarenko, N.A.; Bobik, T.V.; Smirnov, I.V.; Bacheva, A.V.; et al. Immunoproteasome Enhances Intracellular Proteolysis of Myelin Basic Protein. Dokl. Biochem. Biophys. 2013, 453, 300–303.
21. Kim, J.K.; Mastronardi, F.G.; Wood, D.D.; Lubman, D.M.; Zand, R.; Moscarello, M.A. Multiple Sclerosis: An Important Role for Post-Translational Modifications of Myelin Basic Protein in Pathogenesis. Mol. Cell. Proteom. 2003, 2, 453–462.
22. Kuzina, E.S.; Kudriaeva, A.A.; Glagoleva, I.S.; Knorre, V.D.; Gabibov, A.G.; Belogurov, A.A. Deimination of the Myelin Basic Protein Decelerates Its Proteasome-Mediated Metabolism. Dokl. Biochem. Biophys. 2016, 469, 277–280.
23. Harauz, G.; Musse, A.A. A Tale of Two Citrullines—Structural and Functional Aspects of Myelin Basic Protein Deimination in Health and Disease. Neurochem. Res. 2007, 32, 137–158.
24. Wang, C.; Neugebauer, U.; Bürck, J.; Myllykoski, M.; Baumgärtel, P.; Popp, J.; Kursula, P. Charge Isomers of Myelin Basic Protein: Structure and Interactions with Membranes, Nucleotide Analogues, and Calmodulin. PLoS ONE 2011, 6, e19915.
25. Kuzina, E.; Kudriaeva, A.; Smirnov, I.; Dubina, M.V.; Gabibov, A.; Belogurov, A. Glatiramer Acetate and Nanny Proteins Restrict Access of the Multiple Sclerosis Autoantigen Myelin Basic Protein to the 26S Proteasome. BioMed Res. Int. 2014, 2014, 926394.
26. Belogurov, A.; Kuzina, E.; Kudriaeva, A.; Kononikhin, A.; Kovalchuk, S.; Surina, Y.; Smirnov, I.; Lomakin, Y.; Bacheva, A.; Stepanov, A.; et al. Ubiquitin-Independent Proteosomal Degradation of Myelin Basic Protein Contributes to Development of Neurodegenerative Autoimmunity. FASEB J. 2015, 29, 1901–1913.
27. Sutherland, B.W.; Toews, J.; Kast, J. Utility of Formaldehyde Cross-Linking and Mass Spectrometry in the Study of Protein–Protein Interactions. J. Mass Spectrom. 2008, 43, 699–715.
28. Klockenbusch, C.; Kast, J. Optimization of Formaldehyde Cross-Linking for Protein Interaction Analysis of Non-Tagged Integrin β 1. J. Biomed. Biotechnol. 2010, 2010, 1–13.
29. Szklarczyk, D.; Gable, A.L.; Nastou, K.C.; Lyon, D.; Kirsch, R.; Pyysalo, S.; Doncheva, N.T.; Legeay, M.; Fang, T.; Bork, P.; et al. The STRING Database in 2021: Customizable Protein-Protein Networks, and Functional Characterization of User-Uploaded Gene/Measurement Sets. Nucleic Acids Res. 2021, 49, D605–D612.
30. Szklarczyk, D.; Gable, A.L.; Lyon, D.; Junge, A.; Wyder, S.; Huerta-Cepas, J.; Simonovic, M.; Doncheva, N.T.; Morris, J.H.; Bork, P.; et al. STRING V11: Protein-Protein Association Networks with Increased Coverage, Supporting Functional Discovery in Genome-Wide Experimental Datasets. Nucleic Acids Res. 2019, 47, D607–D613.